MethodsX 7 (2020) 101117

Contents lists available at ScienceDirect

MethodsX

journal homepage: www.elsevier.com/locate/mex

Method Article

Application of a flexible polymer microECoG array to map functional coherence in schizophrenia model

F.Z. Fedor[a,b,d], A Zátonyi[b,c,d], D. Cserpán[f], Z. Somogyvári[f], Z. Borhegyi[e], G. Juhász[e], Z. Fekete[c,d,*]

[a] Doctoral School of Chemical Engineering and Material Sciences, Pannon University, Veszprém, Hungary
[b] ELTE NAP Neuroimmunology Research Group, Department of Biochemistry, Institute of Biology, Eötvös Loránd University, Budapest, Hungary
[c] Centre for Energy Research, Hungarian Academy of Sciences, Budapest, Hungary
[d] Research Group for Implantable Microsystems, Faculty of Information Technology & Bionics, Pázmány Péter Catholic University, Budapest, Hungary
[e] Department of Biochemistry, Eötvös Loránd University, Budapest, Hungary
[f] Theoretical Neuroscience and Complex Systems Research Group, Department of Computational Sciences, Wigner Research Centre for Physics, Budapest, Hungary

A B S T R A C T

Anatomically, connections form the fundamental brain network, functionally the different types of oscillatory electric activities are creating a temporarily connected fraction of the anatomical connectome generating an output to the motor system. Schizophrenia can be considered as a connectome disease, in which the sensory input generates a schizophrenia specific temporary connectome and the signal processing becomes diseased showing hallucinations and adverse behavioral reactions. In this work, flexible, 32-channel polymer microelectrode arrays fabricated by the authors are used to map the functional coherence on large cortical areas during physiological activities in a schizophrenia model in rats.

- Fabrication of a flexible microECoG array is shown.
- Protocol to use a flexible microECoG is demonstrated to characterize connectome diseases in rats.
- Customized method to analyze the functional coherence between different cortical areas during visually evoked potential is detailed.
- R-based implementation of the analysis method is presented.

* Corresponding author.
E-mail address: fekete.zoltan@itk.ppke.hu (Z. Fekete).

https://doi.org/10.1016/j.mex.2020.101117

ARTICLE INFO
Method name: Cortical coherence mapping in connectome diseases
Keywords: Electrocorticography, Connectome disease, EEG, Brain mapping, Neuroimaging, Schizophrenia
Article history: Received 11 February 2020; Accepted 19 October 2020; Available online 22 October 2020

Specifications table

Subject Area:	Neuroscience
More specific subject area:	*Neuroengineering*
Method name:	*Cortical coherence mapping in connectome diseases*
Name and reference of original method:	*If applicable, include full bibliographic details of the main reference(s) describing the original method from which the new method was derived.*
Resource availability:	https://bitbucket.org/csdori/brainarear/src/master/

Method details

Fabrication of a microelectrode array

Polymer ECoG arrays of 32 recording channel has 4 × 8 site configuration with 300 µm' site diameter and 1 mm inter-site distance. The fabrication of the polymer based array relies on MEMS (micro-electro-mechanical systems) processes utilizing photolithography, thin film deposition and dry etching steps [6]. The advantage of the approach is that it can be upscaled to human and macaque studies [7,13,14] and can potentially be combined with other neuroimaging techniques [19,20]. A 4″ silicon substrate is used as handle wafer throughout the micromachining process. After dipped into 1:20 hydrogen-fluoride solution, the wafer is coated by 4 µm' thick polyimide (PI2611, HD Microsystems GmbH, Germany) layer. Hardbake of the layer was performed at 300 °C for 60 min on a 200 CBX hotplate (Brewer Science, US) after a softbake process at 130 °C for 3 min. The patterning of the metallization layer was based on lift-off process. 300 nm aluminum layer was e-beam evaporated and etched via a photoresist mask (Microposit 1818, Rohm and Haas Company, USA). 15 nm TiOx and 270 nm platinum was sputtered on the aluminum/photoresist double layer in a DC magnetron sputtering machine (Leybold GmbH, Germany) in a single vacuum cycle. After the deposition step, the photoresist and the aluminum was removed in acetone and in Al etchant (mixture of phosphoric, nitric and acidic acid), respectively. A 4 µm thick second layer of polyimide as a top passivation layer was spin-coated and baked on top of the metallization. The opening of the recording sites, pads and releasing of the PI/Pt/PI structure was performed by reactive ion etching in $CF_{4/}O_2$ plasma (gas ratio was 1:1) in an Anelva DEA 506 reactive ion etching equipment (Anelva Corporation, USA) at 300 W power through a 100 nm aluminum evaporated hard mask. After RIE etching, the Al mask was removed in Al etchant and the released arrays were simply peeled off the wafer mechanically by lab tweezers. The pads in the backbone of the ECoG structures are soldered on a 2 × 16 channel PreciDiP electrical connector (Preci-dip SA, Switzerland) at 265 °C using Sn/Ag soldering alloy.

Figs. 1,9

The impedance of electrophysiological recording sites was measured by electrochemical impedance spectroscopy (EIS) in a three electrode compartment in physiological saline using an Ag/AgCl reference electrode and a platinum wire as a counter electrode. Reference 600 (Gamry Instruments, PA, USA) potentiostat, Gamry Framework 6.02 and Echem Analyst 6.02 were used for experimental control, data collection and analysis. Experiments were performed in a Faraday cage. The probe signal was sinusoidal, with an RMS value of 25 mV. Assessment of the electrochemical stability of the flexible neural interface is provided in Fig. 2a. To evaluate coherence between cortical structures, it is essential to record intracranial EEG with microarrays of low variability in impedance. Soaking the polyimide based interface in phosphate buffered saline for several days at a bath temperature of 37 °C is a typical procedure to evaluate the structural integrity of the ECoG device. In our case (16 days of soaking), after two days, the average impedance at 1 kHz was found relatively stable, and the low standard

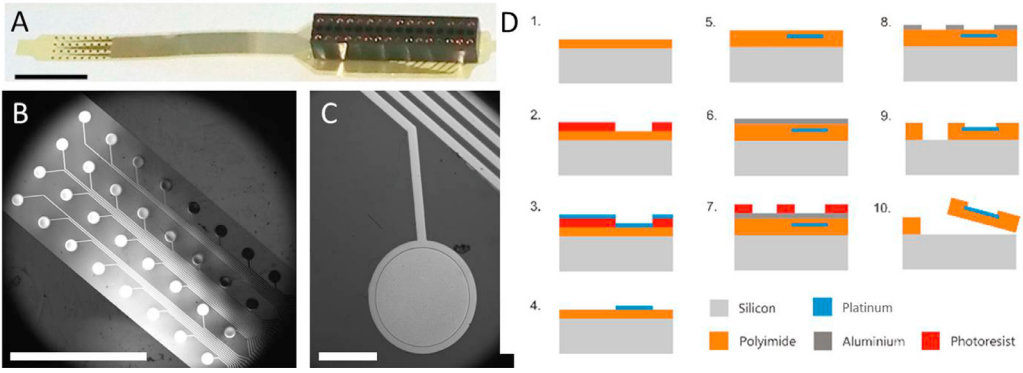

Fig. 1. (a) Photo of the ready to use microECoG array. Close microscopic view on a 32-channel sensor array (b) and on a platinum recording site (c). Scale bars show10 mm, 0.5 mm and 150 µm, respectively. Schematics on the manufacturing process of the microdevice (d).

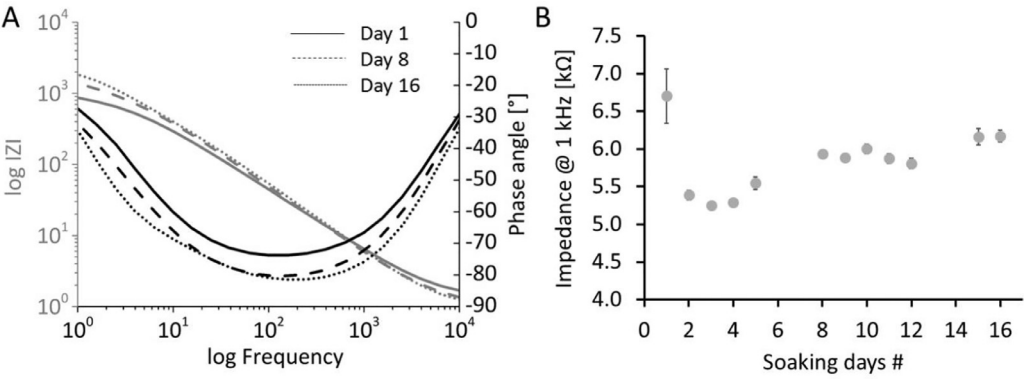

Fig. 2. (a) Impedance of a representative recording site plotted against frequency measured by electrochemical impedance spectroscopy. (Z @ 1 kHz = 5.39 +- 0.065 kOhm) and (b) Change of average impedance of all recording sites at 1 kHz along the course of 16-day long soaking test.

deviation among individual recording sites makes the device suitable to measure coherence between cortical areas.

Surgery

Wistar rats (350–500 g) were used in this study. The animals were housed in groups of 2–4 per cage (diurnal cycle, lights on from 9:00 to 18:00), with ad libitum access to food pellets and water. Rats were anaesthetized with Isoflurane (0.5–1%, Forane, Abbott), and mounted in a stereotaxic frame. The skull was exposed and cleaned, then skull bone was thinned to provide a suitable surface for the electrode implantation. Three stabilizing screws were fixed around the thinned bone surface at anterior, posterior, and medial directions while a reference plate is placed under the skin in front of the left ear (Fig. 3/A). The thin bone surface was folded up (toward the medial direction) without the harm of the dura mater and the electrode was positioned so that all of the contacts had direct contact with the brain surface (Fig. 3/B). The 25th contact was positioned 0.5–1 mm lateral in line with the Bregma and the longitudinal axis of the assembly was parallel to the mid-sagittal line. After the proper positioning of the electrode assembly the bone was folded back to the top of the electrode to give protection and insulation (Fig. 3/C). UV-bound cement (TetricEvoFlow,

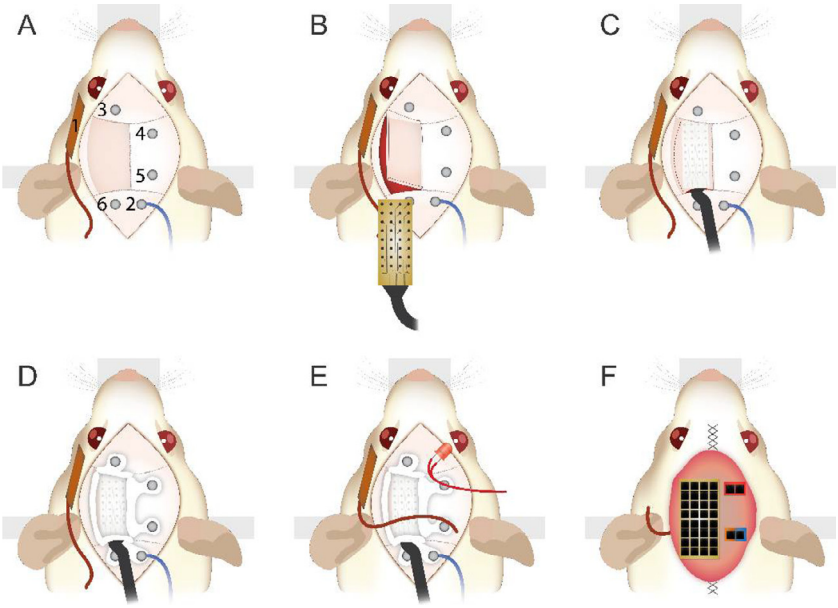

Fig. 3. The method of electrode implantation. The stabilizing screws (3,4,5,6) are arranged around the electrode assembly while the reference plate (1) is placed in front of the left ear. A screw ground electrode (2) was placed above the cerebellum.

IvoclarVivadent; Liechtenstein) was used to stabilize the bone surface above the foil electrode and the skull was covered by dentacrylic cement (GC America Inc., USA) which also held the sockets and covered the screws (Fig. 3/D). A screw ground electrode was placed above the cerebellum. A 5 mm diameter red LED (Bright LED Honkong Ltd.) was placed retrobulbally as a light source and had minimal contact with the tissue [17] (Fig. 3/E). After surgery, antibiotics were given to the animal (2,5% Baytril, Bayer Hungária Ltd., Hungary). Animals were allowed to recover at least for 3 days after implantation.

Electrophysiological validation

During the experiments, animals ($n = 11$) were housed in 12–12 h of light-dark cycle using 500 lux light. Electrophysiological measurements were made in a closed Faraday cage in darkness (under 0.17 msd), using a 32 channel Amplipex KJE-1001 (Amplipex Ltd., Hungary) amplifier. The behavior of the animals was recorded with camera and their movements were monitored with a 3D accelerometer (ACC-2x, Supertech Ltd., Hungary). EEG recordings were made on 35 channels (32 for the electrode, and 3 for the accelerometer) at 20 kHz sampling rate using AmpliRec (Amplipex Ltd., Hungary) program for 2 h each. During the stimulation with LED the animal was exposed to a series of 0,2 Hz stimuli after 10 min of dark adaptation. Spike2 (Cambridge Electronics Design Limited, UK) program was used to give stimuli (1 ms wide, 100 / session) via BioStim stimulator (Supertech Ltd., Hungary). Ketamine (Calypsol, in 15 mg/kg or 50 mg/kg dose) was injected intraperitoneally followed by the recording of the EEG for at least two hours. EEG recording was made on 36 channels (32 for the electrode, 1 for the stimulus events and 3 for the accelerometers) at 20 kHz sampling rate using AmpliRec (Amplipex Ltd., Hungary) program. The basic timeline of the experiments was the following: after a minimum of 3 days' recovery period control recordings were made with and without visual stimulation for 2–2 h. The control recordings were followed by recording with ketamine injection when recording with visual stimulations was also made. At the end of the experiments, the animals were anaesthetized, perfusions were made, and their brains were removed for further research. LFP

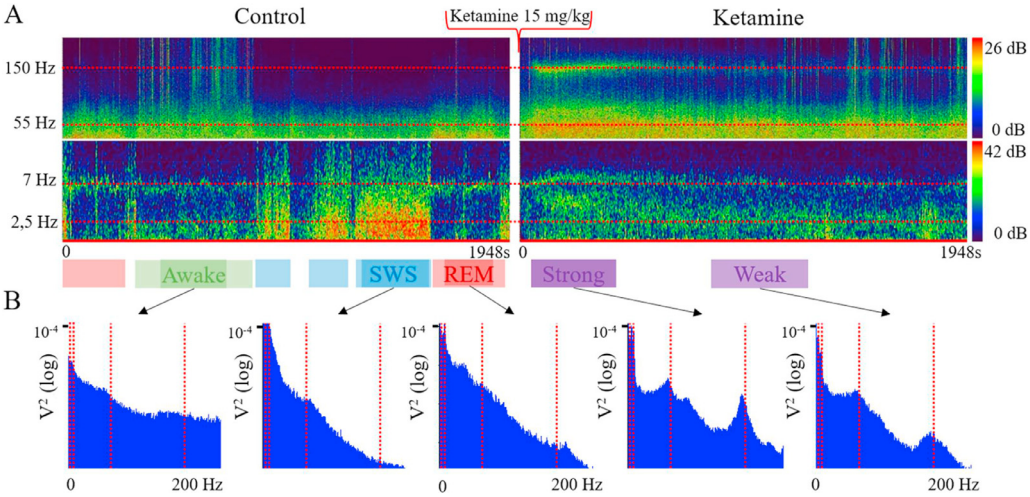

Fig. 4. The spectral comparison of normal EEG with ketamine induced EEG. Sonograms (A) of control and ketamine injected (15 mg/kg) state are shown on top left and right panes. Red lines label the middle of those EEG frequency ranges that showed clear disturbances in response to ketamine. Below the Control sonogram color coded areas label the identified behavioral states (Green – Awake; Blue – Slow wave sleep; Red – REM sleep), and darker areas indicate the parts used in analyses. Purple areas label the time ranges after ketamine injection also used in analyses (Str. – Strong (early) ketamine effect; Weak (late) ketamine effect). Panel B shows the power density spectra of the labeled time ranges on logarithmic scale and the dashed red lines labels the same frequencies than on the sonograms. The sonograms were made with Spike 2 (upper two: top dB – 26, range dB – 24, block size – 8192; lower two: top dB – 42, range dB – 24, block size - 32,768).

preprocessing was made, the input signal went through a DC offset subtraction and low-pass filtering at 200 Hz, then data analysis was performed (1.4 Data analysis).

Ketamine schizophrenia model

Schizophrenia is a chronic disease that has both negative (affective flattening, alogia, avolition, anhedonia, and attentional impairment) and positive (prominent delusions, hallucinations, positive formal thought disorder, and persistently bizarre behavior) aspects [1]. To observe this phenomenon, an animal model is needed that can imply transient cognitive and behavioral symptoms that mimic those observed in schizophrenic patients. NMDA receptor antagonists such as ketamine applied in subanesthetic dose induce symptoms of schizophrenia in humans and animals [10]. Schizophrenia is also characterized by abnormalities in gamma oscillations. In the gamma frequency range, ketamine enhances both background, evoked power, and induces spontaneous high-frequency oscillations as well [16]. Brain diseases are based on the pathologically altered functional connectome resulting pathological outputs to physiological input. Ketamine injection in subanesthetic dose is introduced as a model of human schizophrenia based on its marked antagonistic action on NMDA receptors including the receptors of the fast spiking cortical interneurons [3,9].

After control period, low dose (15 mg/kg IP.) ketamine injection was performed inducing schizophrenia-like state. In control and ketamine treated animals visually evoked potentials (VEP) were recorded to measure the visual data processing. Comparing the phase and power relationship between the two groups of data the nature of ketamine induced schizophrenia-like states were disclosed and then validated with the normal states (awake, slow wave sleep, REM sleep) (Fig. 4.). The spectral analysis of data showed distinct peaks after ketamine injection that lasted but gradually disappeared as the time passed. Beside the characteristic high frequency oscillation around 150 Hz, other EEG bands were also affected. Further investigation of the observed peaks (Figs. 5 and 6) was made to reveal the spectral changes over the cortical surface and the significance level of the changes. While gradual power changes were dominating during the normal states of the rat, after ketamine

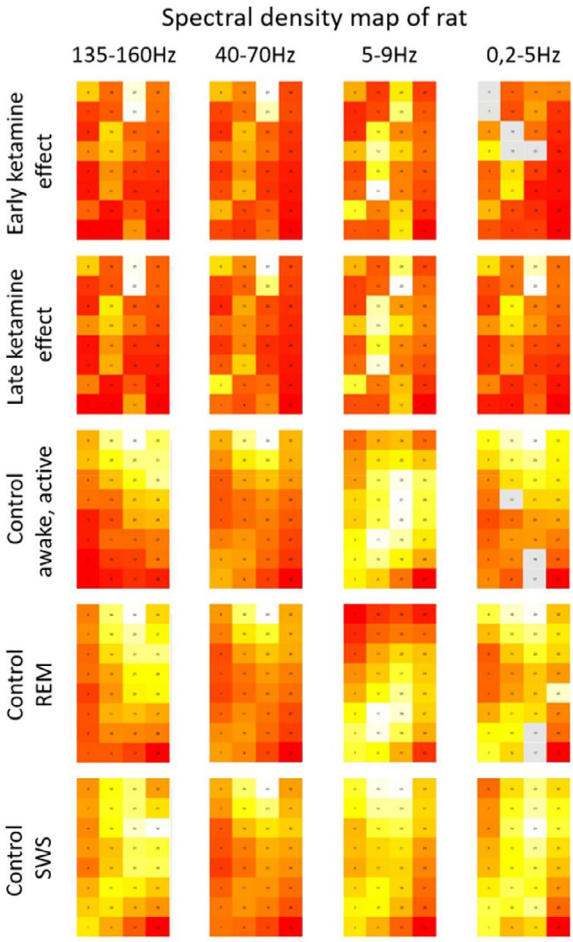

Fig. 5. The power spectrum values of four EEG frequency bands (columns: 135–160 Hz, 40–70 Hz, 5–9 Hz, 0,2–5 Hz) were calculated and color-coded to show their distribution over the rat's cortical surface in different normal brain states (rows: Awake, REM sleep, Slow wave sleep) and after ketamine injection.

injection the cortical distribution showed a rather fragmented, mosaic-like picture which coincides with the behavioral changes and the literature as the rat was visibly disoriented.

Data are analyzed with coherence mapping combined with advanced 2 dimensional kernel current source density analysis. High stability in different EEG synchronization states and during ketamine effect was revealed. The pattern of high coherence cortical sites is corresponding to the anatomically identified functional brain areas of the rat brain. Multichannel coherence analysis also allowed to demonstrate the connectome changes in different vigilance states of the rat. Flash induced VEP as a stimulus driven form of connectivity controlling mechanism also showed reproducible changes under ketamine application (Fig. 6).

To further quantify the changes in the cortical information flow induced by ketamine application, we measured the delay of the VEP response appearance. We have calculated the cross-correlation functions between mean VEP responses for all channel pairs and defined the delays as the positions of the maxima of the cross-correlation functions. Based on these delays, we concluded, that the earliest (and strongest) response appears on channel 30 in correspondence with its anatomical position in the

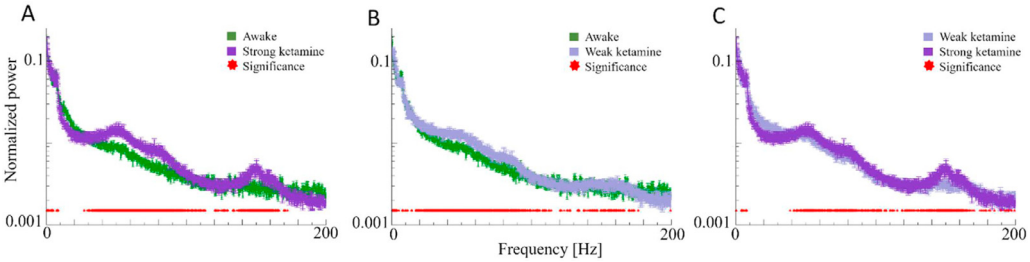

Fig. 6. Normalized power spectra comparison are presented. Awake activity is compared with strong (A) and weak (B) ketamine effect. On panel C the different degrees of ketamine effect are compared. Red stars indicate the sections where there is a significant difference between the two sections at $p = 0.05$ significance level with Bonferoni correction (2000 frequency value, 10 state comparison). Averages are calculated from 30, 10 s long data for each state and their Standard Error of Mean (SEM) are shown.

Figure 6. Visually evoked potentials from 32 channels (0,2 Hz, 1 ms wide LED flash behind contralateral eye bulb) were averaged from control as well as ketamine injected state of a rat. Panel A shows responses from 8 example channels (their position is shown on the satellite image), control (blue) and ketamine injected states (red) are overlapped. kCSD plots in 4–4 time windows (5 s wide) are visible on panel B and C. The intensity of color follows the intensity of brain activity (current sinks are marked with red while current sources are blue). While panel B shows control, panel C shows ketamine effect, numbers are corresponding to the indicated points of recording on the left panel. Coherences (on the right of panel B and C) were calculated from a 5 s long time window in the 0–200 Hz frequency range. Different clusters are marked by arbitrary colors on the maps, while the intensity of the colors and the numbers in the rectangles represents the strength of the affiliation to the actual cluster. Note the differences in the spreading of the VEP on the kCSD and the delicate differences on the coherence map.

V1 (Fig 7). Comparing to the channel 30, the delay increased up to 50 ms at the most medio-rostral and the medio-caudal channels in the control case. This resulted a concentric pattern of increasing delays, which is a characteristic signal of the wave-like propagation of the VEP response through the whole measured part of the cortex (Fig 7, B). Parallel to the increasing delay, the peak correlation decreases from close-to-one values to 0.4 (Fig 7, C). After ketamine administration, the amplitudes of the evoked potential were smaller, but still clear signs of the VEP response were observable on many channels. In contrast to the control case, the maxima of the cross-correlation functions were at 0 ms for almost all channels, relative to the channel 30, after ketamine administration (Fig 7, D and E). The peaks of the cross correlation functions were higher for most of the channels, but the wave-like propagation was not observable through the cortex, the responses appear in synchrony on almost all channels.

Data analysis

We validated our method on simulated data. Each channel out of the 32 is constructed as a sinusoidal oscillation of either 5, 25, 30, 80, 90 Hz representing the different clusters. Each cluster contains at least 3 channels of the same frequency, but the initial phase was set differently. Our algorithm identified the exact same clusters as in the ground truth as shown on Fig. 8.

Source localization

Local synaptic currents generate spatially widespread LFP distributions, according to the Poisson-equation. The aim of the current source density analysis is to calculate the spatial distribution of the summed synaptic currents based on the measured LFP signals. This inverse problem is underdetermined if the LFP does not known in 3D with the spatial resolution comparable of the sources. In order to get a well-defined solution, different Current Source Density (CSD) analysis methods apply different assumptions. Here we applied the kernel Current Source Density (kCSD, [12]) method, which is well suited to the geometry of the 2D grid measurements. It assumes, that the current sources form Gaussian shaped source blobs under the plane of the electrode grid, thus it describes well any smoothly changing source distributions. Different versions of the method were developed to adopt the different measurements with 1D, 2D and 3D electrode systems and different

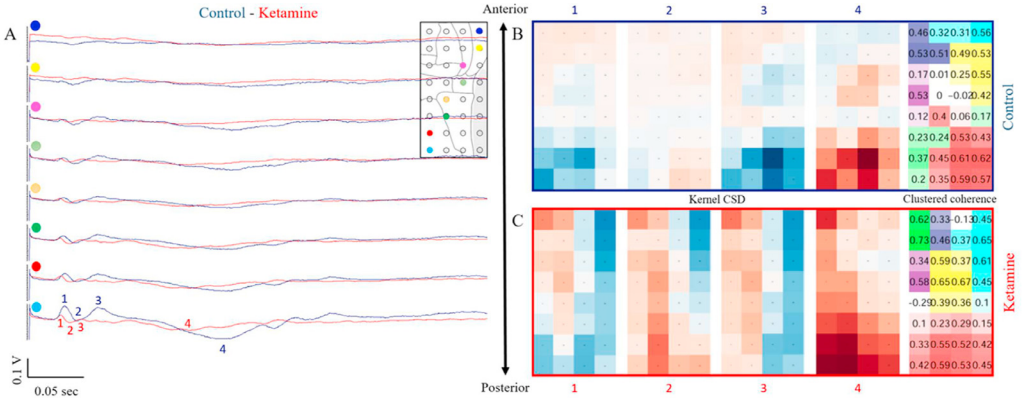

Fig. 7. Propagation of the VEP response through the cortex in control and ketamine treated periods. A and D: Cross-correlation functions (colored lines) between mean VEP responses (400 ms) on channel 30 (insert, black star) and 8 chosen channels through the whole diagonal of the electrode grid (insert, colored dots) during control periods (A) and after ketamine treatment (D). The peaks of the cross-correlation functions shift and attenuate by the increasing distance from the V1 cortex in the control case, but there are no signs of shifting peaks in the ketamine treated case and the attenuation is less pronounced. The position of the peaks define the characteristic delay of the information flow from the visual cortex. B and E: The delay values color coded for all channels. The earliest (and strongest) response appeared on the channel 30 (black star) and the delay increased up to 50 ms at the most medio-rostral and the medio-caudal channels in the control case (B). The concentric pattern of the increasing delays is the hallmark of the wave-like propagation through the cortex in the control case. In contrast, VEP responses appear in synchrony on almost all channels after ketamine treatment, without delays or signs of the propagation (E). C and F: The peak correlation values decrease by the increasing cortical distance in both control and ketamine treated cases, but correlation is higher with most channels in the ketamine case (F). White numbers on panel C correspond to the functionally different cortical areas: 1 –Primary somatosensory cortex, forelimb region; 2 –Primary somatosensory cortex, hindlimb region; 3 –Primary motor cortex; 4 –Secondary motor cortex; 5 –Primary somatosensory cortex; shoulder region; 6 –Primary somatosensory cortex, trunk region; 7 –Lateral parietal association cortex; 8 -Medial parietal association cortex; 9 –Primary visual cortex; 10 –Secondary visual cortex.

source distributions, or even to make it applicable to single neurons with known morphology [5]. The resulted distribution of current sources is less spatially correlated, than the LFP was and it helps the identification and localization of the synaptic activity.

Coherence analysis

Coherence can be interpreted as a measure, which informs about how much populations are co-working. Between two series, a value close to 1 means very similar patterns with a certain delay in time, a value close to 0 means negligible relationship. For the purpose of estimating relationships between populations, it is possible to select either the extracellular potentials or the kCSD values. Calculating the coherence between all the kCSD values related to the population of neurons close to the certain electrodes resulted in a table, the coherence matrix, informing about the similarities between the functional behavior of the neuron populations.

Coherence clustering

The electrode channels, belonging to one functionally connected area are determined by a clustering algorithm, in which the coherence was utilized as a pair-vise similarity measure.

This method assumes, that channel pairs which show high coherence, characteristic to the tight phase relation between the two kCSD time series, are functionally connected and belong to one functional unit. Thus, functional units can be revealed by clustering the channels into highly coherent clusters. Coherence clustering was initially applied to reveal and distinguish hippocampal subfields and synaptic layers, as well as areas and granular, infra- and supragranular layers in the neocortex [4].

Using the coherence as similarity, partitioning around medoids clustering algorithm was applied to reveal coherent clusters. The clusterings were run by different cluster numbers, from 2 to 20 and

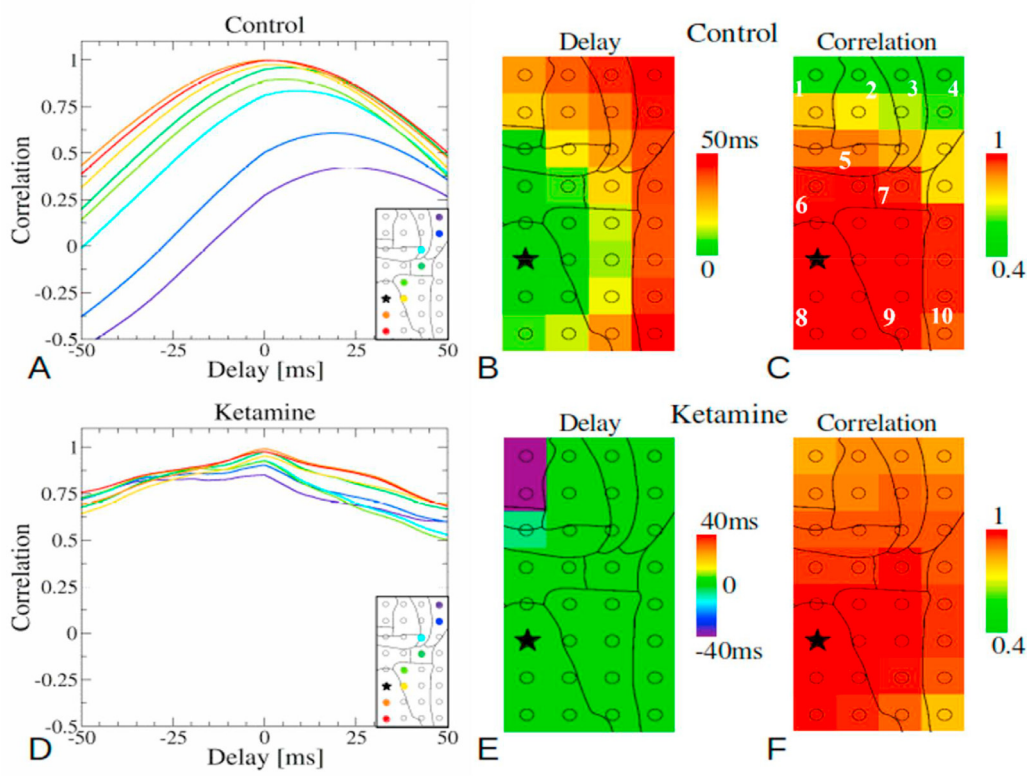

Fig. 8. Validation of the coherence clustering algorithm on simulated data. a)-h) The channels are arranged in a grid shape and are allocated to different clusters as the cluster number changes. The clusters are shown by various colours, the saturation and the numbers at the channel locations show the silhouette value to describe how similar this channel is to its cluster. i) The spatial distribution of the 5 clusters, the blue, magenta, red and yellow clusters correspond to the 30, 80, 5, 90, 25 Hz frequency signals respectively. j) We selected the optimal cluster number based on the highest value of the average silhouette width. As expected, in this case the optimal cluster number is 5, the method performed well on this dummy data by finding the correct clusters. k) The silhouette width for each cluster changes as the number of clusters increases, in case of 5 clusters all the silhouette values are high.

the optimal number of clusters were determined by measuring the quality of the resulted clusters, in terms of average silhouette width.

Description of the program used for analysis: BrainAreaR

BrainAreaR is a software with graphical user interface developed in R [2]. Besides generating images of simple quantities as raw and filtered data, power and frequency spectrum, kernel source density distribution map and coherence is also calculated. One of the main features is the coherence-clustering which can be used for identifying functionally cohesive neuron population.

Step 1 - Loading the data. After selecting the data file, the sampling frequency and the time range of the recording will be detected, an option to load only part of the data is available as well. Certain channels might be discarded from the further analysis, which can be useful in case of damaged electrodes, which will be marked by red crosses on the electrode distribution map.

Step 2 - Scouting. A simple view of the raw filtered data is provided for a certain time window and channel on the second tab. 5 frequency bands are shown and amplitude scaling is provided. This figure is intended to help the filtering of the data.

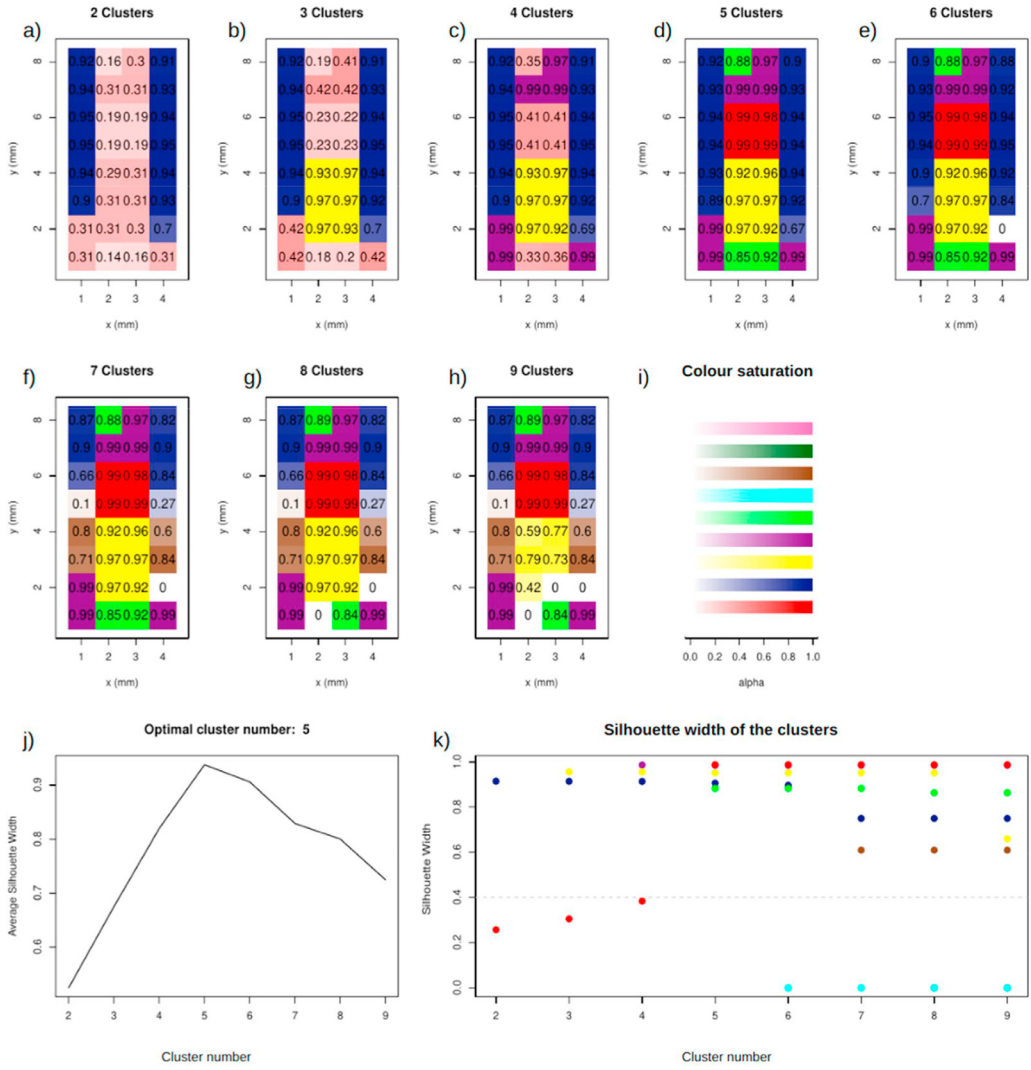

Fig. 9. Flowchart diagram of the data processing steps. First, we performed frequency filtering on the selected data interval based on the frequency band of interest. Then the kernel current source density value is calculated from the filtered potential. As a next step, the coherence value is calculated between each pair of channels. We cluster into varying number of clusters the pairwise coherence values by using the partitioning around medoids algorithm. The optimal number of clusters are selected based on the highest average silhouette width value of the clusters.

Step 3 - Filtering. A frequency range of interest can be selected on the next panel and the spectral density related to each channel will appear on separate figures. The peaks of different frequencies in case of the simulated data are clearly visible. In case of the experimental data the frequency spectrum of an awake animal shows the typical drop of intensity at higher frequencies, on some channels a peak at 40–60 Hz regime can be observed.

Step 4 - Activity maps. A color-coded spatial distribution of the potential and kCSD values, as this latter is a more direct measure of the underlying neural mechanisms at a certain timestep is displayed

on the next tab [12]. By selecting arbitrary instants in time or downloading a short video along time might help in observing spatial pattern formation and propagation.

Step 5 – Coherence clustering. By applying the partitioning around medoids clustering algorithm we aimed to identify the functionally cooperating brain areas [8]. The reasonable number of clusters were selected by the average silhouette a width measure. Global and local maxima values were considered as meaningful for indicating the number of optimal clusters with an expectation to be greater than 0.4. The resulted map of functional brain areas might be used for estimating the anatomical brain areas and show changes in electrophysiological behavior due to various brain states or drugs. Validating the method on the simulated data it is visible, that the channels group according to their frequencies and the silhouette width measure finds the optimal number of clusters. In case of the experimental data, based on the recordings of an awake animal 6 clusters were found to be optimal, which could be identified with the V1, V2, S1, M, MPta and LtA cortical areas.

Conclusions

Extracellular events can be measured with several techniques from simplest handcrafted multiple screw electrode arrangement to epi–cranial electrodes, glued multi-electrode assembly or complex prefabricated thin layer multi-electrode assemblies such as ours [13,15,18]. One of the major advantages of the polymer ECoG array is the potential of recording from multiple functionally different cortical areas at the same time invasively from the cortical surface and non-invasively from the skull and the possibility to detect brain oscillations as well as synchronization. The simple handcrafted screw electrodes can harm the cortical surface and their relative position is not constant, their number is limited. The number and the position of recording sites of the polymer array are freely variable, the polymer layer can be made transparent and it can easily be combined with other measuring techniques such as optical imaging [21]. Our array can be freely placed to the cortical surface or to the skull, it follows surface changes. It is able to detect brain waves of freely moving rats similarly to the human EEG mapping technologies [11]. Revealing functional connectivity and its changes are often central questions in electrophysiological investigations of the brain. This requires the delineation of different brain areas as well as a proper measure of functional connectivity between them. Coherence clustering is a unique approach, which solves these two problems in parallel: it utilizes the similarity measure to define functional units on the brain surface, while able to track the changes of the connection structure as well. Furthermore, visualizing the connection structure of brain areas is not a straightforward problem. As coherence clustering offers a clear representation of the connection structure, it could be useful for exploratory data analysis. Ketamine had serious effects on signal propagation in rat brain and our electrode foil was shown to be a reliable tool to investigate changes in these spatio-temporal patterns of electric signals. Smaller number of spatially more extent clusters in optimal coherence clustering, as well as higher cross correlations showed higher and wider synchronization in the cortex, resulted by ketamine administration. Parallel, the normal propagation pattern of visually evoked responses were impaired, showing that the normal chain of information transmission between brain areas during visual information processing is blocked by the ketamine as well. Combined with the presented analytical tool this method is suitable for translational studies on animal models of schizophrenia and the results are comparable with the data obtained on human subjects. Our present technology provided an excellent translational tool for schizophrenia research and drug development.

Acknowledgments

The supportive work of the cleanroom staff at the Microsystems Laboratory of the Hungarian Academy of Sciences is highly appreciated. This work was supported by the Hungarian Brain Research Program (2017-1.2.1-NKP-2017-00002 to F. Z. F., Z. S. and Z. F.) the National Research, Development and Innovation Office (Grants: NKFIH K 120143, K 113147) and FIEK_16-1-2016-0005 grant to Zs. B. and G. J. The support of the European Union through the grant EFOP-3.6.3-VEKOP-16-2017-00002 co-financed by the European Social Fund is also acknowledged. The Bolyai János Scholarship of the

Hungarian Academy of Sciences and Scholarship of the New National Excellence Foundation (UNKP-19-4-PPKE-9) granted for Z. F. is also acknowledged. The research was supported by the Human Brain Project associative grant CANON (NN118902). The authors also wish to thank the supportive graphical work of Vilmos Tóth.]

Declaration of Competing Interest

The authors declare that they have no known competing financial interests or personal relationships that could have appeared to influence the work reported in this paper.

References

[1] N.C. Andreasen, S. Olsen, Negative v positive schizophrenia: definition and validation, Arch. Gen. Psychiatry 39 (7) (1982) 789–794.
[2] BrainAreaR code (2019): https://bitbucket.org/csdori/brainarear/src/master/.
[3] A. Becker, B. Peters, H. Schroeder, T. Mann, G. Huether, G. Grecksch, Ketamine-induced changes in rat behaviour: a possible animal model of schizophrenia, Prog. Neuropsychopharmacol. Biol. Psychiatry 27 (4) (2003) 687–700.
[4] Berényi A., Somogyvári Z., Nagy A., Roux L., Long J., Fujisawa S., Stark E., Leonardo A., Harris T. and Buzsáki Gy Large-scale, high-density (up to 512 channels) recording of local circuits in behaving animals. J. Neurophysiol. 111 (5) (2014) 1132–1149, doi:10.1152/jn.00785.2013.
[5] D. Cserpán, D. Mészena, L. Wittner, K. Tóth, I. Ulbert, Z. Somogyvári, D. Wójcik, Revealing the distribution of transmembrane currents along the dendritic tree of a neuron with known morphology from extracellular recordings, Elife 6 (2017) e29384, doi:10.7554/eLife.29384.
[6] Z. Fekete, A. Pongrácz, Multifunctional soft implants to monitor and control neural activity in the central and peripheral nervous system: a review, Sens. Actuat. B-Chem. 243 (2017) 1214–1223.
[7] B.A. Hollenberg, C.D. Richards, R. Richards, D.F. Bahr, D.M. Rector, A MEMS fabricated flexible electrode array for recording surface field potentials, J. Neurosci. Methods 153 (1) (2006) 147–153.
[8] L. Kaufman, P.J. Rousseeuw, Finding Groups in Data: an Introduction to Cluster Analysis, 344, John Wiley & Sons, 2009.
[9] B. Kocsis, R.E. Brown, R.W. McCarley, M. Hajos, Impact of ketamine on neuronal network dynamics: translational modeling of schizophrenia-relevant deficits, CNS Neurosci. Ther. 19 (6) (2013) 437–447.
[10] J.H. Krystal, L.P. Karper, J.P. Seibyl, G.K. Freeman, R. Delaney, J.D. Bremner, ..., D.S. Charney, Subanesthetic effects of the noncompetitive NMDA antagonist, ketamine, in humans: psychotomimetic, perceptual, cognitive, and neuroendocrine responses, Arch. Gen. Psychiatry 51 (3) (1994) 199–214.
[11] D. Lehmann, Human scalp EEG fields: evoked, alpha, sleep, and spike-wave patterns, in: Synchronization of EEG Activity in Epilepsies, Springer, Vienna, 1972, pp. 307–326.
[12] J. Potworowski, W. Jakuczun, S. Łęski, D. Wójcik, Kernel current source density method, Neural Comput. 24 (2) (2012) 541–575.
[13] B. Rubehn, C. Bosman, R. Oostenveld, P. Fries, T. Stieglitz, A MEMS-based flexible multichannel ECoG-electrode array, J. Neural Eng. 6 (3) (2009) 036003.
[14] Karl A. Sillay, Paul Rutecki, Kathy Cicora, Greg Worrell, Joseph Drazkowski, Jerry J. Shih, Ashwini D. Sharan, Martha J. Morrell, Justin Williams, Brett Wingeier, "Long-term measurement of impedance in chronically implanted depth and subdural electrodes during responsive neurostimulation in humans, Brain Stimul. 6 (5) (2013) 718–726, doi:10.1016/j.brs.2013.02.001.
[15] P. Słowiński, L. Sheybani, C.M. Michel, M.P. Richardson, C. Quairiaux, J.R. Terry, M. Goodfellow, Background EEG connectivity captures the time-course of epileptogenesis in a mouse model of epilepsy, eNeuro 6 (4) (2019).
[16] K.M. Spencer, M.A. Niznikiewicz, M.E. Shenton, R.W. McCarley, Sensory-evoked gamma oscillations in chronic schizophrenia, Biol. Psychiatry 63 (8) (2008) 744–747.
[17] O. Szabó-Salfay, J. Pálhalmi, E. Szatmári, P. Barabás, N. Szilágyi, G. Juhász, The electroretinogram and visual evoked potential of freely moving rats, Brain Res. Bull. 56 (1) (2001) 7–14.
[18] C. Wu, M. Wais, E. Sheppy, M. del Campo, L. Zhang, A glue-based, screw-free method for implantation of intra-cranial electrodes in young mice, J. Neurosci. Methods 171 (1) (2008) 126–131.
[19] A. Zátonyi, Z. Borhegyi, M. Srivastava, D. Cserpán, Z. Somogyvári, Z. Kisvárday, Z. Fekete, Functional brain mapping using optical imaging of intrinsic signals and simultaneous high-resolution cortical electrophysiology with a flexible, transparent microelectrode array, Sens. Actuat. B 273 (2018) 519–526.
[20] Zátonyi, M. Madarász, Á. Szabó, T. Lőrincz, R. Hodován, B. Rózsa, Z. Fekete, Transparent, low-autofluorescence microECoG device for simultaneous Ca2+ imaging and cortical electrophysiology in vivo, J. Neural Eng. (2020) in press, DOI:, doi:10.1088/1741-2552/ab603f.
[21] Zátonyi, Zs. Borhegyi, M. Srivastava, D. Cserpán, Z. Somogyvári, Z. Kisvárday, Z. Fekete, Functional brain mapping using optical imaging of intrinsic signals and simultaneous high-resolution cortical electrophysiology with a flexible, transparent microelectrode array, Sens. Actuat. B-Chem. 273 (2018) 519–526.